Comparative evaluation of structure-borne noise transfer paths in a laboratory experiment

Akira Inoue,[a] Seungbo Kim,[a] and Rajendra Singh[b]

(Received 2006 January 12; revised 2006 July 04; accepted 2006 July 04)

This article examines structure-borne noise transfer paths by conducting a laboratory experiment with simulated source and receiver chambers. First, two indirect estimation methods for dynamic path (interfacial) forces are utilized to rank order paths from 100 to 2800 Hz. Estimated forces are also compared with direct force measurements made using impedance heads. Next, four alternate methods that estimate partial sound pressures in the receiver room are investigated as path measures. These include mobility or impedance formulation with either measured path forces or velocities. Finally, path power quantifiers (such as un-weighted or weighted mean-square force or velocity) are investigated, though some negative values are found in calculations. The center path dominates over a broad frequency range especially when the measured force is used along with the mobility formulation. Nevertheless, its dominance is not as clear when the measured velocity is used with the same formulation. Further, the rank order changes when the impedance formulation is employed although the total sound pressures remain the same. Our paper has demonstrated that an experimental study alone (without any rotational measurements) could lead to an ambiguous or inconsistent rank order in some cases and thus some caution must be exercised. ***© 2006 Institute of Noise Control Engineering.***

Primary subject classification: 43; Secondary subject classification: 74.8

1 INTRODUCTION

Structure-borne noise in many practical systems including ground vehicles is transmitted through multiple parallel paths that include machinery mounts, vibration isolators and structural connections or joints. Proper rank ordering of structural paths is crucial for the design process since significant dynamic interactions among paths may occur.[1,2] The precise role of structural paths is not well documented although the isolation effect of mounts has been well studied.[3–5] Further, multiple paths and their interactions may exhibit distinct characteristics from a single path system.[4–6] The transfer path analysis (TPA) technique rank orders dominant vibration transmission paths, based on measured frequency response functions (FRF) and operational data.[7–11] This analysis requires knowledge of the interfacial path forces and then relating them to partial sound pressures at a receiver location. However, a direct measurement of in situ dynamic forces in a practical system is very difficult. Consequently, an indirect force estimation scheme must be employed.[11–14] The power flow concept has also been used to determine the vibration transmission efficiency of several systems.[15–18] Nevertheless, power flow through a particular path in a multi-path problem may inherently assume negative values, which would make the analysis troublesome. To address some of these issues, we employ a laboratory source-path-receiver experiment. The chief objectives of this article are as follows. 1. Develop experimental procedures to evaluate the structure-borne noise transfer path measures. 2. Examine the indirect methods that estimate interfacial paths forces and partial sound pressures at the receiver. 3. Compare the structure-borne noise path rank ordering schemes based on some direct measurements and several indirect estimations. The scope of this study is limited to the frequency domain analysis of a linear time-invariant system, from

[a] Acoustics and Dynamics Laboratory, Dept. of Mechanical Engineering and Center for Automotive Research, The Ohio State University, 201 West 19th Ave. Columbus, OH 43210.

[b] Acoustics and Dynamics Laboratory, Dept. of Mechanical Engineering and Center for Automotive Research, The Ohio State University, 201 West 19th Ave. Columbus, OH 43210; email: singh.3@osu.edu

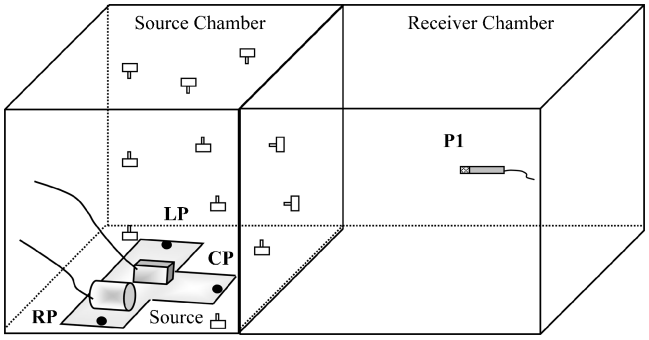

Fig. 1—Schematic of the experimental two-chamber system. Vibration from the source unit is transmitted to the receiver microphone location P1 as structure-borne noise through three hard paths (mounts); left, center and right paths are denoted as LP, CP and RP respectively. Many accelerometers are installed in walls of the source chamber.

100 to 2800 Hz. Only the translational motions are considered, and thus the multi-dimensional rotational effects would not be included.[19–22]

2 EXPERIMENTAL SYSTEM AND TYPICAL MEASUREMENTS

Figure 1 shows the experimental system that consists of source and receiver chambers. A motor-air pump unit is fixed to a T-shape plate, as shown in Fig. 2. Both motor and pump act as the vibration sources, but each source can be separately operated and controlled, and thus they could be uncorrelated. The T-shaped plate (with sources) is mounted within the source chamber by three hard mounts or the impedance heads that measure path forces and accelerations. The structure-borne vibration is transmitted through three parallel mount paths then to the base of the source chamber,

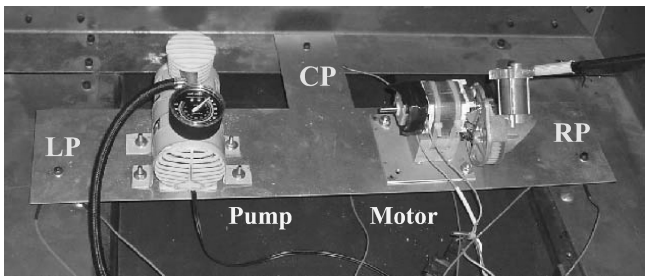

Fig. 2—Source unit consisting of an air pump, a motor and a T-shaped base plate. This unit is installed near the floor of the source chamber base plate using three mounts (or paths LP, CP and RP).

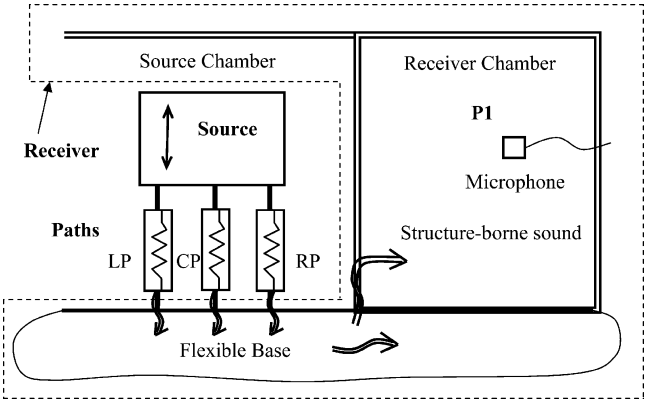

Fig. 3—Structure-borne noise transmission paths of the experimental system. Left, center and right paths are connected to the source chamber base plate via hard mounts. Receiver is denoted by the dotted line.

and is finally transmitted into the receiver chamber. Three microphones are installed in the receiver chamber to measure the sound pressures. The source chamber is open on the left side in order to conduct the impact hammer testing (for the acquisition of transfer functions), but the receiver chamber is closed to minimize any air-borne noise paths. The concept of source-path-receiver is also illustrated in Fig. 3, where the structure-borne noise receiver (consisting of a portion of the source chamber and receiver chamber) is denoted by the dotted lines. Our article focuses on the role of three mount paths to the partial sound pressures at a receiver location. Note that we will primarily deal with force and motion variables at path interfaces (at the base of the source chamber or input to the receiver).

The motor or air pump can be operated at 6 different speeds, including the zero speed for each. Therefore, the source unit has 36 discrete speed combinations. Overall, 48 accelerometers (in the source chamber), 3 microphones (in the receiver chamber) and 3 impedance heads (at the path points) are used. The source chamber has 5 sheet metal surfaces since the left side is open, and thus 9 accelerometers are installed on each surface except the bottom surface; further, 3 impedance heads are located at the path mounting points. Thus, indirect methods would employ accelerations at 3 or 48 points in the source chamber to estimate the path forces. Note that in the operational experiment, vibrations are generated by uncorrelated pump and motor only; no shaker or impact hammer is applied to the source unit when the sources are operated. The impedance heads measure interfacial forces and accelerations in only the vertical direction. Forces and path motions in other directions are not considered here. The

maximum number of channels for each measurement set is 15, and the operational structural responses at the left path (LP) are synchronized for establishing a reference for all record sets. Thus consistent phase relations are maintained for the entire measurement sets. Only one microphone (at P1 as shown in Fig. 1) is utilized for the analysis reported in this article.

First, the impact (modal) test is conducted to obtain the vibro-acoustic transfer functions of the two-chamber system. For this test, the motor-pump unit is disconnected from the source room structure and an impulsive force is applied at each path (mounting point). The accelerometers and the microphones measure the following frequency response functions on a narrow band basis from 100 to 2800 Hz: Accelerance a/F (m/s^2N) and acoustic-structural function p/F (Pa/N) where a is the complex-valued structural acceleration amplitude, F is the complex-valued force amplitude and p is the complex-valued sound pressure amplitude in the receiver chamber. The circular frequency (ω) dependence (in rad/s) is dropped from all frequency domain expressions since it is ubiquitous. The accelerance a/F spectrum is then converted to the mobility V/F transfer function (in the frequency domain) by using $a=j\omega V$ where j is the imaginary unit and V is the complex-valued velocity amplitude. Second, the motor and the air pump are operated after the source unit is installed. The impedance heads, as well as the accelerometers and the microphones, measure the operational responses. Such direct measurements will be compared with the indirect estimations. Finally, by using the above mentioned measured data, the paths are rank ordered by the indirectly estimated forces, partial sound pressures, power flow and weighted mean-square force or velocity calculations. Typical measured spectra, in terms of structural and acoustic frequency response functions and sound pressures, are shown in Figs. 4 and 5 respectively. As evident from Fig. 4, the narrow band spectrum clearly shows resonances and anti-resonances even at those frequencies where the coherence (not shown in this article) is less than perfect. Fig. 5 shows the sound pressure at receiver location P1 when the source unit is operated at five different levels. Only the analyses with the highest source excitations (level 5 in Fig. 5) are presented in the subsequent sections of this paper.

3 INDIRECT METHODS OF ESTIMATING PATH FORCES

The direct measurement of the interfacial path forces in many practical systems is difficult if not impossible. Consequently, the path forces would need

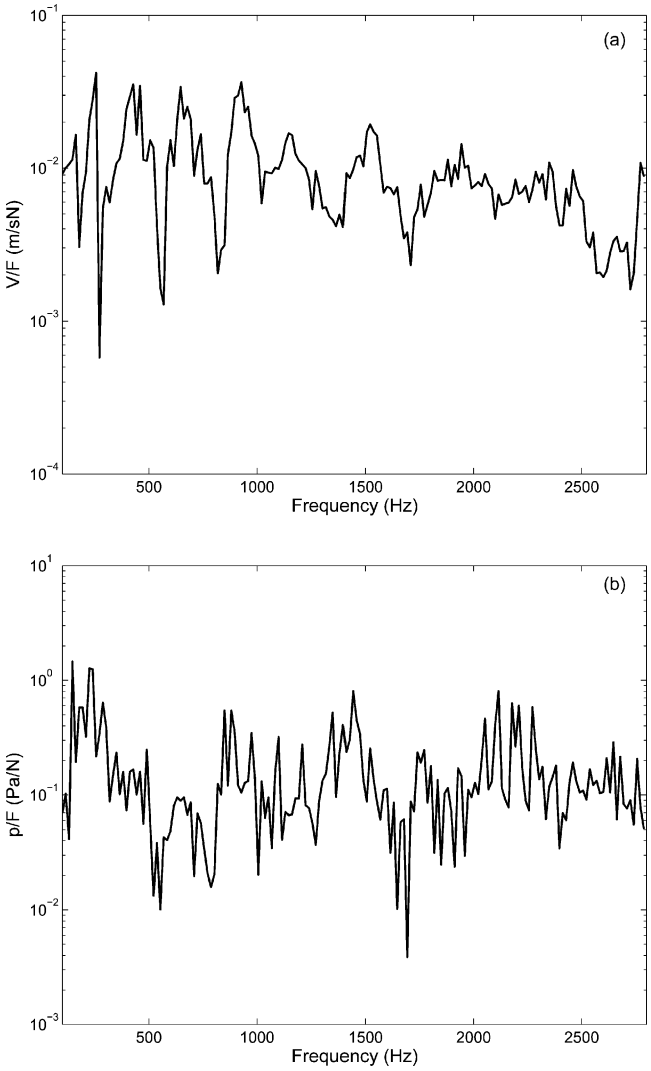

Fig. 4—Measured structural and acoustic frequency response functions (FRF) on a narrow band basis: (a) driving point mobility at the left path; (b) acoustic FRF (p/F) with sound pressure in the receiver room (at P1) and force at the center path.

to be estimated via an indirect method. We employ two alternate indirect methods to estimate the interfacial path forces. The governing equations of motion in the frequency domain in terms of velocity may be expressed as $\mathbf{F}(\omega)=[\mathbf{F}/\mathbf{V}]\mathbf{V}(\omega)$, where $\mathbf{F}$ is the external force vector, $\mathbf{V}$ is the response velocity vector, and $[\mathbf{F}/\mathbf{V}]=[\mathbf{Z}(\omega)]$ is the impedance matrix. For a discretized system, $[\mathbf{Z}]=[\mathbf{K}/j\omega+j\omega\mathbf{M}+\mathbf{C}]$ where $\mathbf{K}$, $\mathbf{M}$ and $\mathbf{C}$ are stiffness, mass (inertia) and viscous damping matrices, respectively. Since the impedance is usually associated with the blocked (or fixed) boundary conditions that are difficult to implement in practice, define the mobility matrix, $[\mathbf{Y}(\omega)]=[\mathbf{V}/\mathbf{F}]=[\mathbf{F}/\mathbf{V}]^{-1}$, which is associated with the free boundary conditions

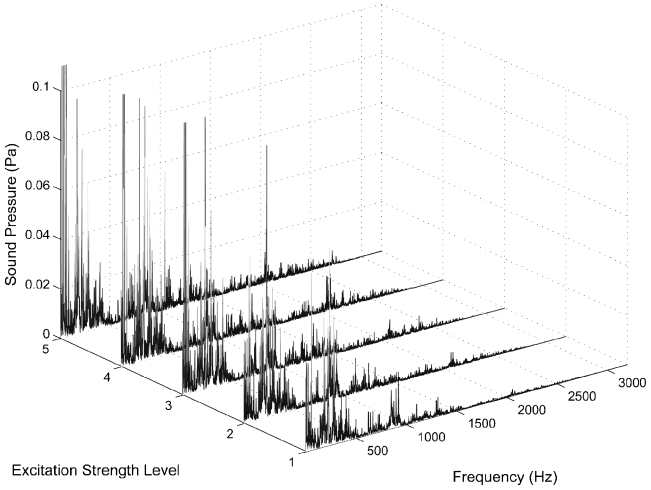

Fig. 5—Sound pressure spectra (on narrow band basis), measured in the receiver room at P1, for 5 excitation levels. Source strength level settings are given by the following combination of voltages (V). Level 1: Pump 2 V*, Motor* 40 V*; Level 2: Pump* 4 V*, Motor* 45 V*; Level 3: Pump* 6 V*, Motor* 50 V*; Level 4: Pump* 8 V*, Motor* 55 V*; Level 5: Pump* 10 V*, Motor* 60 V.

(easy to achieve in experimental studies). Thus, define the path interfacial forces and velocity vectors by the following complex-valued formulation at any frequency where subscripts ℓ and n are the number of responses and path locations, respectively.[14]

$$\mathbf{V}_{l\times 1} = \left[\frac{\mathbf{V}}{\mathbf{F}}\right]_{l\times n} \mathbf{F}_{n\times 1} \tag{1}$$

Equation (1) also defines the forced response ($\mathbf{V}_{\ell\times 1}$) of the linear system when the external harmonic force is applied.

3.1 Indirect Methods I and II

First, only the velocity responses at the driving ends of paths are considered as these can be further related to the structure-borne noise as shown by Singh and Kim.[4] Thus, the interfacial force vector ($\mathbf{F}$ is now used as the path force vector) at any frequency is estimated from Eqn. (1) as follows where $[\mathbf{Z}]$ is the driving point impedance matrix, based on n paths locations.[11–14]

$$\mathbf{F}_{n\times 1} = [\mathbf{Z}]_{n\times n}\mathbf{V}_{n\times 1} = \left[\frac{\mathbf{V}}{\mathbf{F}}\right]^{-1}_{n\times n} \mathbf{V}_{n\times 1} \tag{2}$$

In this article, this force estimation technique is designated as the indirect method I. The structural impedance matrix is obtained via numerically inverting the measured driving point mobility matrix as $[\mathbf{Z}] = [\mathbf{V}/\mathbf{F}]^{-1}$.

Next, the operating structural responses and mobilities at ℓ number of response locations are considered along with the path driving ends. Rewriting Eqn. (2), the interfacial force vector is estimated as follows where the superscript + implies pseudo inverse and T is the transpose.

$$\mathbf{F}_{n\times 1} = \left[\frac{\mathbf{V}}{\mathbf{F}}\right]^{+}_{l\times n} \mathbf{V}_{l\times 1} \tag{3}$$

$$\left[\frac{\mathbf{V}}{\mathbf{F}}\right]^{+}_{l\times n} = \left[\left[\frac{\mathbf{V}}{\mathbf{F}}\right]^{\mathrm{T}}\left[\frac{\mathbf{V}}{\mathbf{F}}\right]\right]^{-1}\left[\frac{\mathbf{V}}{\mathbf{F}}\right]^{\mathrm{T}} \tag{4}$$

In this article, the above mentioned indirect force estimation approach is designated as the indirect method II; it could be referred to as the least-squares method. Further, the mobility matrix $[\mathbf{Y}]=[\mathbf{V}/\mathbf{F}]_{48\times 3}$ is measured at 48 points in the source chamber (including three path mounting points). All spectra are obtained on a narrow band basis from 100 to 2800 Hz. Results are then converted to the one-third octave band spectra for the sake of visual display and clarity.

3.2 Estimated Path Force Results

The interfacial force spectra are estimated for three mount paths by using the above mentioned indirect methods (I and II). Estimations are shown in Fig. 6 and compared with the direct force measurements. It is observed in Fig. 6 that the indirect method I yields a better estimation over a wide range of frequencies than the indirect method II; the results are more pronounced for the left and the right paths. However, the force estimated via the indirect method I for the center path deviates from the measured one up to around 500 Hz, as shown in Fig. 6(b).

Observe that the discrepancy between the direct measurement and indirect estimation of path forces is significant in several one third octave frequency bands. Plausible causes of error include contributions from measurement, signal and data processing and conceptual (formulation) errors. First, the error caused by the sensors (accelerometers, force sensors and microphones) themselves should be of the order of about 1% (or say no worse than +/−2 dB) which is relatively small. Second, the error caused in the matrix inversion process could be theoretically considerable especially when the matrix is ill-conditioned, say at the resonant or anti-resonant frequencies. However, in our case, the condition number[12] is found to be less than 50 over most narrow band frequencies (except at 680 Hz where it is 221). An averaged value of the condition number is 10.1, which should not introduce large error in the inversion process. Third, the ignored motions (such as the rotational ones) could have considerable effect, say

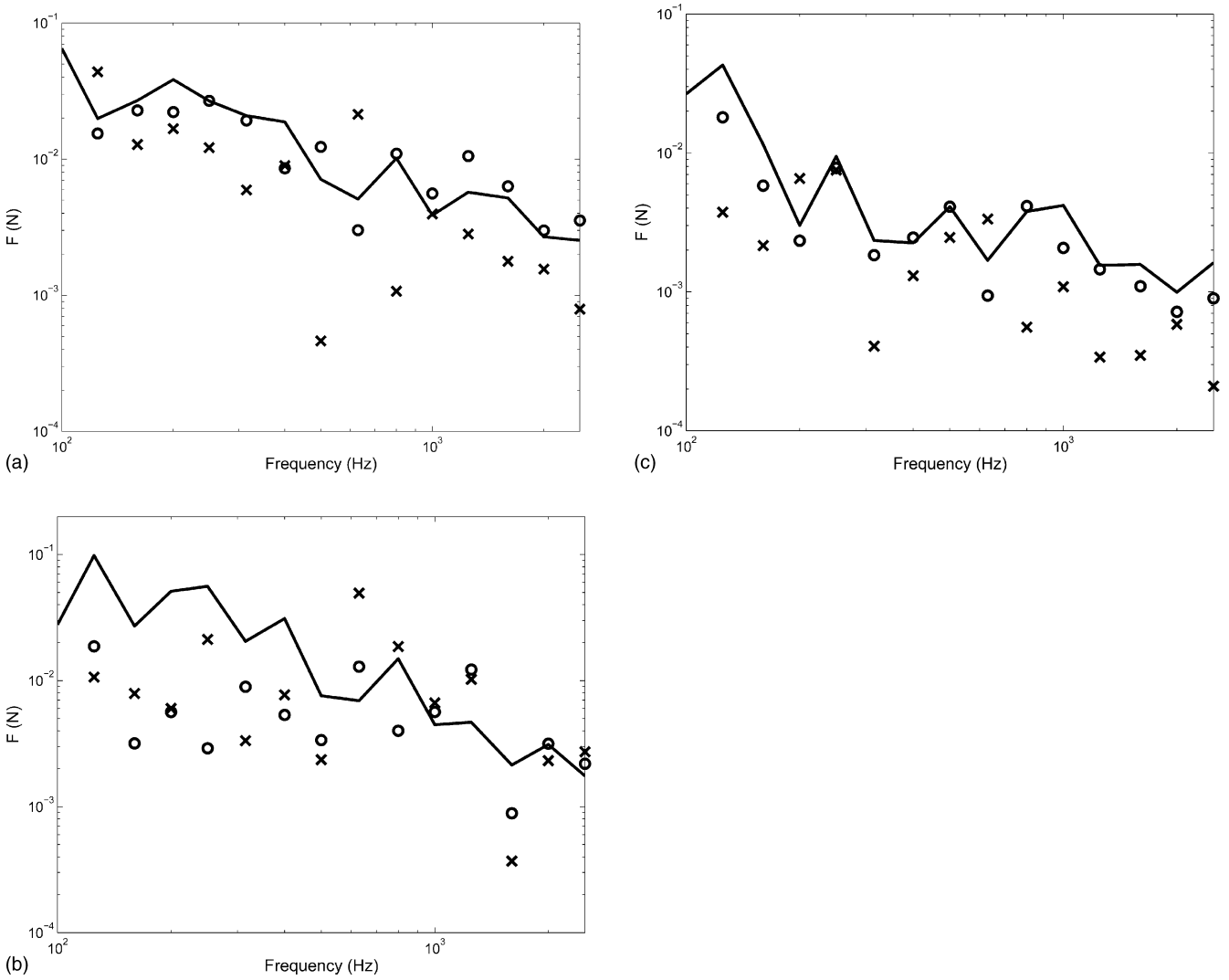

Fig. 6—Interfacial force spectra (on one third octave band basis) for 3 paths: (a) left path; (b) center path; (c) right path. Key: ——, measured (direct) force; o, estimated force via the indirect method I; x, estimated force via the indirect method II.

of the order of discrepancies seen in Fig. 6. We have estimated such errors in a separate article.[11]

4 INDIRECT METHODS OF ESTIMATING PARTIAL SOUND PRESSURES

Four alternate schemes are employed to rank order the structural paths in terms of the partial sound pressure components. First, consider the mobility (Y) and the impedance (Z) formulations, which are denoted in the subscripts. Each is evaluated in terms of the measured force (F) or the measured velocity (V), as denoted in the subscript. The four competing formulations are defined below where the complex-valued p is the total (or partial) sound pressure amplitude in the receiver room (at P1) at given frequency, i is the path index, and the superscripts m and e denote measured and estimated quantities, respectively.

$$p_{\mathrm{FY}}(\omega)=\sum_{i=1}^{3}p_{\mathrm{FY,i}}=\sum_{i=1}^{3}\left[\frac{p}{F_i}\right]F_i^{\mathrm{m}}=\left[\frac{\mathbf{p}}{\mathbf{F}}\right]_{1\times 3}\mathbf{F}_{3\times 1}^{\mathrm{m}} \quad (5)$$

$$\begin{aligned}p_{\mathrm{FZ}}(\omega)&=\sum_{i=1}^{3}p_{\mathrm{FZ,i}}=\sum_{i=1}^{3}\left[\frac{p}{V_i}\right]V_i^{\mathrm{e}}=\left[\frac{\mathbf{p}}{\mathbf{V}}\right]_{1\times 3}\mathbf{V}_{3\times 1}^{\mathrm{e}}\\&=\left(\left[\frac{\mathbf{p}}{\mathbf{F}}\right]_{1\times 3}\left[\frac{\mathbf{V}}{\mathbf{F}}\right]_{3\times 3}^{-1}\right)\left(\left[\frac{\mathbf{V}}{\mathbf{F}}\right]_{3\times 3}\mathbf{F}_{3\times 1}^{\mathrm{m}}\right)\end{aligned} \quad (6)$$

$$\begin{aligned}p_{\mathrm{VY}}(\omega)&=\sum_{i=1}^{3}p_{\mathrm{VY},i}=\sum_{i=1}^{3}\left[\frac{p}{F_i}\right]F_i^{\mathrm{e}}=\left[\frac{\mathbf{p}}{\mathbf{F}}\right]_{1\times 3}\mathbf{F}_{3\times 1}^{\mathrm{e}}\\&=\left[\frac{\mathbf{p}}{\mathbf{F}}\right]_{1\times 3}\left(\left[\frac{\mathbf{V}}{\mathbf{F}}\right]_{3\times 3}^{-1}\mathbf{V}_{3\times 1}^{\mathrm{m}}\right)\end{aligned} \quad (7)$$

$$p_{VZ}(\omega)=\sum_{i=1}^{3}p_{VZ,i}=\sum_{i=1}^{3}\left[\frac{p}{V_i}\right]V_i^{m}=\left[\frac{\mathbf{p}}{\mathbf{V}}\right]_{1\times3}\mathbf{V}_{3\times1}^{m}$$
$$=\left(\left[\frac{\mathbf{p}}{\mathbf{F}}\right]_{1\times3}\left[\frac{\mathbf{V}}{\mathbf{F}}\right]_{3\times3}^{-1}\right)\mathbf{V}_{3\times1}^{m} \quad (8)$$

In the sound pressure estimation process, only the indirect method I is used to estimate the interfacial path force vector $\mathbf{F}^e$ that corresponds to Eqn. (2). Note that $p_{FY}=p_{FZ}$ and $p_{VY}=p_{VZ}$, though their components are generally different as $p_{FY,i}\neq p_{FZ,i}$ and $p_{VY,i}\neq p_{VZ,i}$. For example, Eqns. (7) and (8) are further expanded as follows.

$$p_{VY}=p_{VZ}=\left(\frac{p}{F_1},\frac{p}{F_2},\frac{p}{F_3}\right)\begin{pmatrix}\frac{F_1}{V_1}&\frac{F_1}{V_2}&\frac{F_1}{V_3}\\ \frac{F_2}{V_1}&\frac{F_2}{V_2}&\frac{F_2}{V_3}\\ \frac{F_3}{V_1}&\frac{F_3}{V_2}&\frac{F_3}{V_3}\end{pmatrix}\begin{pmatrix}V_1\\V_2\\V_3\end{pmatrix} \quad (9)$$

where

$$p_{VY,i}=\frac{p}{F_i}\left\{\frac{F_i}{V_1}V_1+\frac{F_i}{V_2}V_2+\frac{F_i}{V_3}V_3\right\} \quad (10)$$

$$p_{VZ,i}=\left\{\frac{p}{F_1}\frac{F_1}{V_i}+\frac{p}{F_2}\frac{F_2}{V_i}+\frac{p}{F_3}\frac{F_3}{V_i}\right\}V_i \quad (11)$$

Figure 7 shows typical sound pressures (at P1 in the receiver room) as estimated by the indirect methods based on either measured force or velocity formulations given by Eqns. (5) to (8). It is seen that the total sound pressure at any frequency is given by the vector-sum of partial sound pressures by Eqns. (5) and (6), or Eqns. (7) and (8). These estimations are compared with the direct measurements of sound pressures. Although some errors are observed, the estimated pressures match well with the measured ones over a broad range of frequencies. However, the sound pressures that are estimated based on the measured force data differ considerably from the direct measurements up to 300 Hz. Again, the multi-dimensional motions should be considered for a better estimation. In fact, the path ranks might change if all motions (three translations and three rotations at any given measurement location) were to be somehow available.[11]

When the indirect method II (the least-squares technique based on pseudo inverse) is used instead of the indirect method I, we replace $[\mathbf{V}/\mathbf{F}]_{3\times3}^{-1}$ and $\mathbf{V}_{3\times1}^{m}$ with $[\mathbf{V}/\mathbf{F}]_{48\times3}^{+}$ (as defined by Eqn. (4)) and $\mathbf{V}_{48\times1}^{m}$, respectively. Note that p_{VZ} is now expressed by a summation of 48 terms.

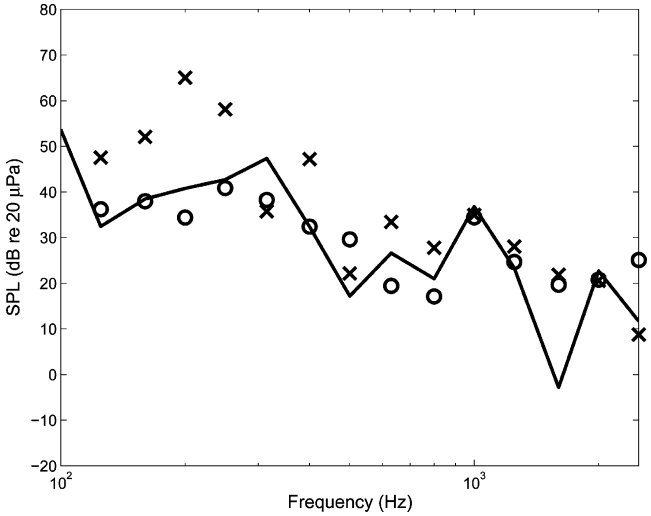

Fig. 7—Receiver room sound pressure levels (SPL) on one third octave band basis. Key: ——, measured (direct) SPL; x, estimated SPL ($p_{FY}=p_{FZ}$) using indirect method based on measured forces ((5) or (6)); o, estimated SPL ($p_{VY}=p_{VZ}$) using indirect method I based on measured velocities ((7) or (8)).

$$p_{VZ}=\sum_{i=1}^{48}p_{VZ,i}=\sum_{i=1}^{48}\left\{\frac{p}{F_1}\frac{F_1}{V_i}+\frac{p}{F_2}\frac{F_2}{V_i}+\frac{p}{F_3}\frac{F_3}{V_i}\right\}V_i \quad (12)$$

If the above mentioned 48 terms could represent contributions to the total sound pressure from each of the 48 structural response points, a comparison of contributions from the three paths may be expanded to a comparison of the 48 response points. Recall that 3 out of the 48 points are the path locations, and thus the other 45 points are on the walls of the source chamber.

5 PATH RANK ORDERS BASED ON PARTIAL SOUND PRESSURES

5.1 Rank Orders Based on Force or Velocity Spectra

Rank orders of paths based on measured forces and velocities are shown in Fig. 8. Measured force spectra show that right path is the weakest and left and center paths are equally dominant, as shown in Fig. 8(a). Unlike the order based on forces, the order of dominance is clear in the velocity spectra over a broad range of frequencies. Figure 8(b) shows that velocity is maximum at the left path and minimum for the center path though most rank orders, as quantified by other path measures, show that the center path is the dominant one. A spectral average of the path forces is

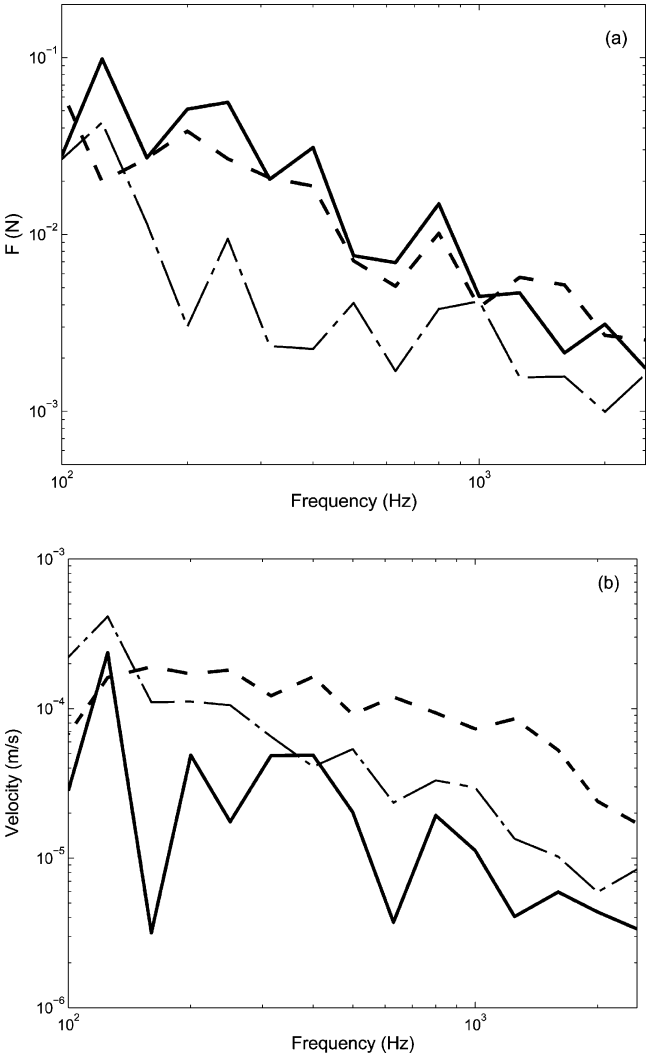

Fig. 8—Measured path force (a) and velocity (b) spectra (on one third octave band basis). Key: - - -, left path; ——, center path; · –· – · –, right path.

calculated, between 100 and 2800 Hz, and these results are listed in Table 1. The averaged results (over the mid-frequency regime) show that the center path is the most dominant of the three in terms of transmitting the force to the receiver. And, the right and left paths seem to transmit almost equal forces to the base.

5.2 Rank Orders Using the Indirect Method Based on Measured Path Forces

The spectral averages of Table 1 (from 100 to 2800 Hz) further compare partial pressure based on the indirect method I (based on the response at 3 points as given by Eqns. (7) and (8)). Mobility and impedance methods yield the same rank orders and both find the center path to be the dominant one. These calculations are repeated for all of the 48 $p_{VZ,i}$ terms as given by the least-squares (the indirect method II, described by Eqns. (3) and (4)). Averaged partial pressures are found to be as follows: 1741 (μPa) for the left path, 1622 (μPa) for the center path and 1492 (μPa) for the right path. When we examine the next 45 points (on the walls), averaged partial pressures from the top 4 response points (on the base panel) are: 856, 714, 689, and 583 (μPa). Observe that 3 path response points (used in indirect method II) contribute much larger pressures (averaged from 100 to 2800 Hz) than the other 45 points on the walls.

Figure 9 shows the partial sound pressure spectra that are estimated by the mobility method given the measured path forces. Overall, the center path is dominant as shown in Fig. 9. Further, in order to compare the partial sound pressures based on the impedance and mobility formulations, the following relative path (partial) pressure level expression (Δp) is defined (in dB) where subscripts i and j are path indices.

$$\Delta p_{i-j} = 20 \log_{10}\left(\frac{|p_i|}{|p_j|}\right), \quad \text{where } i,j = 1,2,3 \qquad (13)$$

Results are shown in Fig. 10 where the measured force is used based on Eqns. (5) and (6). Relative path pressure levels of Fig. 10 show that the path rank orders and their relative strengths are somewhat formulation-dependent. For example, Fig. 10(c) shows that the right path is more dominant than the left path based on the partial sound pressure (around 800 Hz) as estimated by the impedance formulation (6). Conversely, the left path dominates over the right path in the mobility formulation (5) at the same frequency. Nevertheless, the total sound pressures of Fig. 10 from either mobility or impedance formulation should be (and are) identical since $p_{FY}=p_{FZ}$.

5.3 Path Polygons

The partial sound pressure components (at 163 Hz with a frequency resolution of 0.7 Hz) are next represented on the complex plane, allowing us to compare both magnitudes and phases, in Fig. 11 for both mobility and impedance formulations. Figure 11 illustrates that the partial sound pressure components from the three paths constitute the total (estimated) sound pressure but in different ways for the mobility and impedance formulations. Hence, this figure suggests that the partial sound pressure polygon is indeed formulation-dependent. The total sound pressure (the dotted line) is the same, but it is represented by 2 different polygons as is seen in Figs. 11(a) and 11(b), which correspond to the impedance and the mobility formulations, respectively. Many vectorial representations are theoretically possible to describe the same (total) pressure spectrum at an observation point. Nonethe-

Table 1—Spectrally averaged path forces, velocities and partial sound pressures (from 100 to 2800 Hz)

Path Measure	Left Path (LP)	Center Path (CP)	Right Path (RP)
Path Force (N) –Direct Measurement	0.00798 [31%]†	0.02566 [100%] †	0.00800 [31%]†
Structural Velocity at the Receiver End (μm/s)– Direct Measurement	67.08 [179%] †	37.47 [100%]†	73.82 [197%]†
Partial Sound Pressure (dB re 20 μPa) - Indirect Estimation (I) by Mobility Method (Based on Eqn. (7))	38.5 [−2.5 dB]*	41.0 [0 dB]*	39.5 [−1.5 dB]*
Partial Sound Pressure (dB re 20 μPa) – Indirect Estimation (I) by Impedance Method (Based on Eqn. (8))	39.0 [−2.5 dB]*	41.5 [0 dB]*	39.5 [−2.0 dB]*

Key †: Relative value in percent (on a linear basis) compared with the center path
Key *: Relative difference (on a logarithmic basis) compared with the center path.

less, it appears that the mobility type formulation should be preferred since the free boundary conditions are much easier to implement in practice than the blocked boundary conditions. In this paper, only the partial sound pressure magnitudes are considered when comparing the paths. However, their phases should be included in the rank ordering process since out-of-phase relationships cancel out some contributions. For instance, the center path in Fig. 11(a) has a relatively large magnitude, but its phase is 157 degrees relative to the total pressure. If one were to somehow remove this center path (only), the resulting total pressure would be much higher. Similar arguments are applicable to Fig. 11(b).

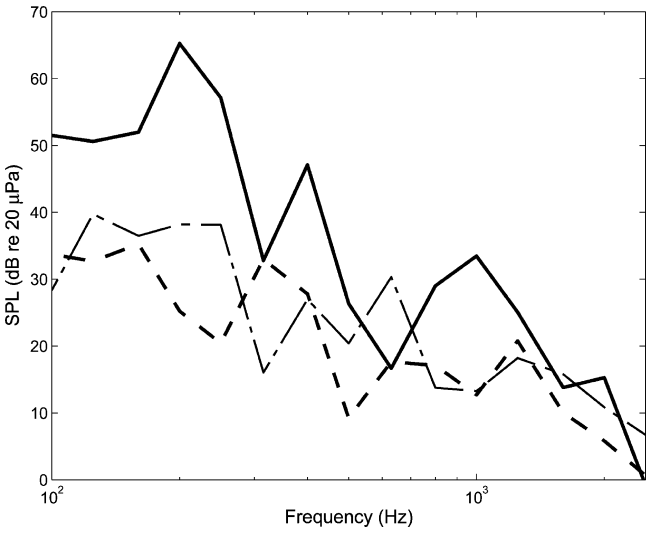

Fig. 9—Estimated partial sound pressures (on one third octave band basis) by using the mobility method with measured forces (5). Key: - - -, left path; —, center path; · – · – · –, right path.

5.4 Rank Orders Using the Indirect Method Based on Measured Path Velocities

Partial sound pressures as estimated with the measured velocities are shown in Fig. 12. Unlike the ones with measured forces of Fig. 9, the center path is not as dominant. And, the right and center paths are somewhat the same up to 200 Hz, as shown in Fig. 12. The spectral averages of partial pressures are tabulated in Table 1. The center path is the most dominant in both estimation methods; and then right and left paths follow respectively. This spectral average is taken from 100 to 2800 Hz since the averaged value suggests the ranking of each path in a clearer or compact manner. It should be noted that the center path is the least dominant based on measured velocities unlike other path rank quantifiers. Further, the total (estimated) sound pressures show somewhat lower magnitudes over

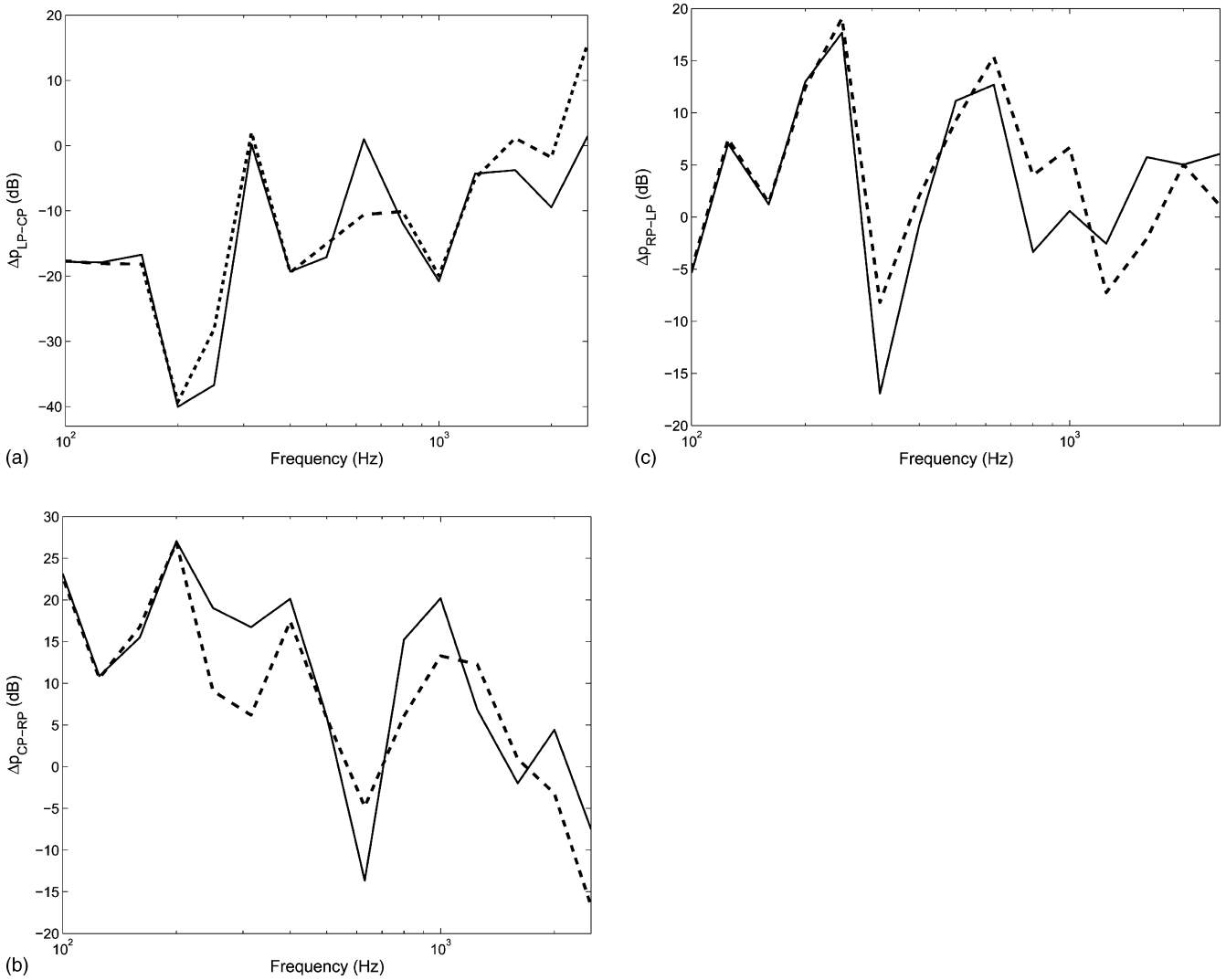

Fig. 10—Relative partial sound pressures (on one third octave band basis) obtained using mobility (5) or impedance (6) method with measured forces: (a) $\Delta p_{\text{LP-CP}}$; (b) $\Delta p_{\text{CP-RP}}$; (c) $\Delta p_{\text{RP-LP}}$. Key: ——, mobility method; - - -, impedance method.

the lower frequency regime, they may be used as path rank quantifiers. Even though the precise role of the structure-borne noise through each path to the partial sound pressure (at a receiver point) is still not clearly understood, our proposed estimation methods (based on the impedance and mobility formulations) should give lead to further refinements.

6 PATH RANK ORDERS BASED ON ENERGY QUANTIFIERS

6.1 Path Rank Order in Terms of Power Flow

The time-averaged vibration power (Π) through a path at any frequency, as defined below, is employed next to rank order the parallel paths.

$$\Pi(\omega) = \frac{1}{2}\,\mathrm{Re}[FV^*] = \frac{1}{2}\,\mathrm{Re}[VF^*] \qquad (14)$$

Here, Re is the real value operator, and superscript * denotes complex conjugation. Note that the active vibration power per cycle represents the dissipated energy under harmonic excitation.[4,23] Unlike the force or velocity vectors, the units of Π (a scalar quantity) are compatible for rotational and translational directions. Therefore, the power flow concept could be easily used. Further, our earlier work shows a close correlation between sound radiation from an 'L' structure receiver to the free field and the vibration power at receiver (driving) points.[4] Vibration powers through three mount paths are obtained by using measured forces and velocities of Fig. 8. Results are shown in Figs. 13(a) and 13(b) for total power and path power components respectively.

The path components of Fig. 13(b) show that the right path is most dominant one from 100 to 250 Hz. Further, Fig. 13(b) shows that the power through the

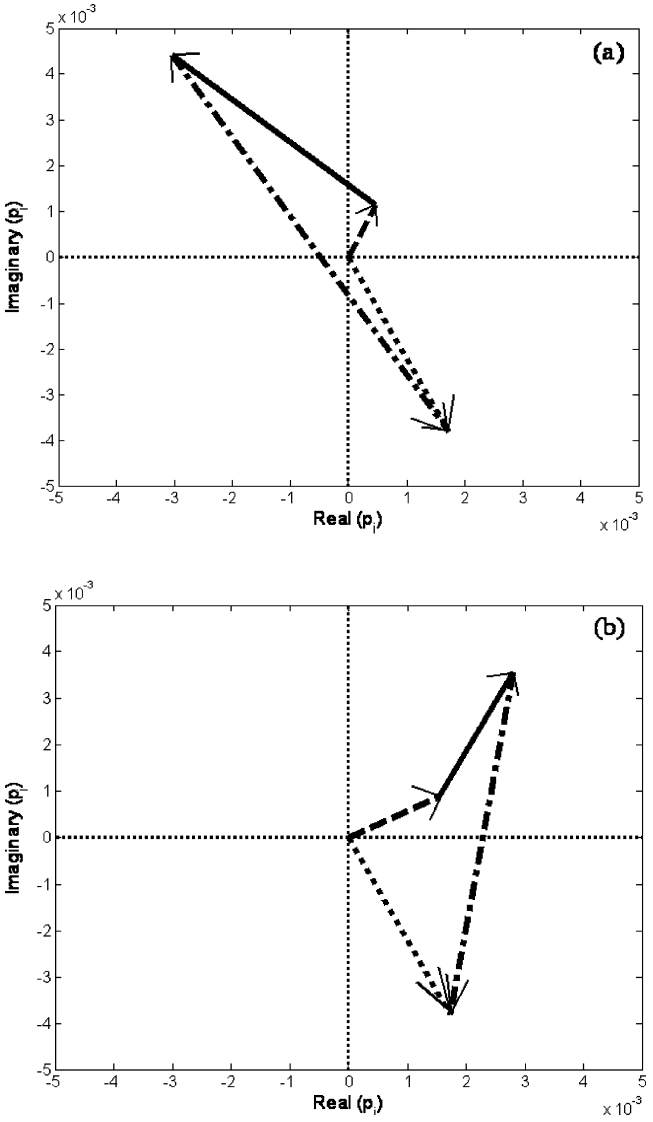

Fig. 11—Vectorial representations of the partial sound pressures at 163 Hz *based on measured velocities:* (*a*) *with impedance method* (*8*)*;* (*b*) *with mobility method* (*7*)*. Key: - - - - - -, total sound pressure, - - -, left path; ——, center path; · – · – · –, right path.*

center path exhibits negative values over a wide range of frequencies, say from 100 to 1000 Hz. Note that the power flow through any path may be negative for the multiple paths case. Negative power flow implies the power flows in a reverse manner, say from receiver to source unit in this case (refer to the article by Singh and Kim[4] for an example of reverse power flow). Further, let us conduct a thought experiment. Consider an analytical uni-axial structure and apply two separate excitations at either ends. No coupling in the system or no physical connection between two independent excitations exists. The vibration power at either end

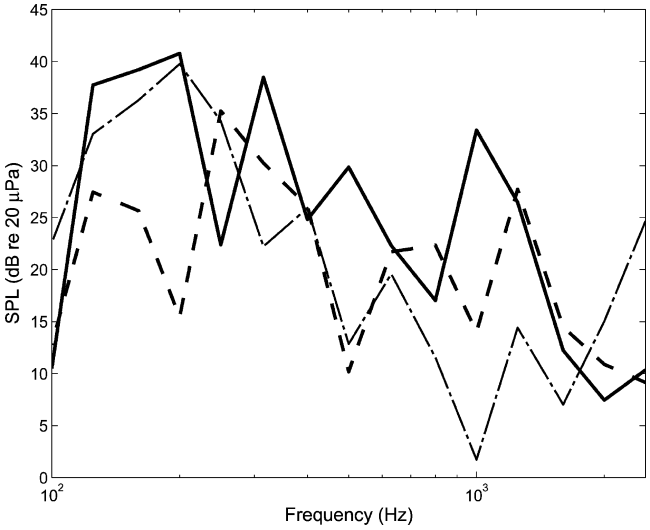

Fig. 12—Path rank orders based on partial sound pressures (*on one third octave band basis*) *obtained via mobility method* (*7*) *with measured velocities. Key: - - -, left path; ——, center path; · – · – · –, right path.*

may become negative although there is no mechanism for energy dissipation beyond the end points. Nonetheless, an interpretation of the negative power flow is somewhat cumbersome, especially in experimental data. The total power should be positive at all frequencies; this is partially seen in Fig. 13(a). Caution must be however exercised since the total power could still be negative for an experimental system especially when some degrees of freedom (especially the rotational motions) are not taken into account, as a negative power is seen at 400 Hz. Again, refer to Ref. 4 for an explanation. Almost all 1/3 octave bands exhibit positive values in Fig. 13(a). The negative value at 400 Hz seems to be due to the missing degrees of freedom.

6.2 Weighted Mean-Square Force and Velocity

First, define the un-weighted mean-square force (Ψ_F^2) and velocity (Ψ_V^2) for uni-directional motions at any frequency as:

$$\Psi_{F,i}^2 = \frac{1}{2}\,\mathrm{Re}[F_i F_i^*] = \frac{|F_i|^2}{2} \tag{15}$$

$$\Psi_{V,i}^2 = \frac{1}{2}\,\mathrm{Re}[V_i V_i^*] = \frac{|V_i|^2}{2} \tag{16}$$

The un-weighted $\Psi_{F,i}^2$ and $\Psi_{V,i}^2$ are generally meaningful for uni-directional motions but their relative

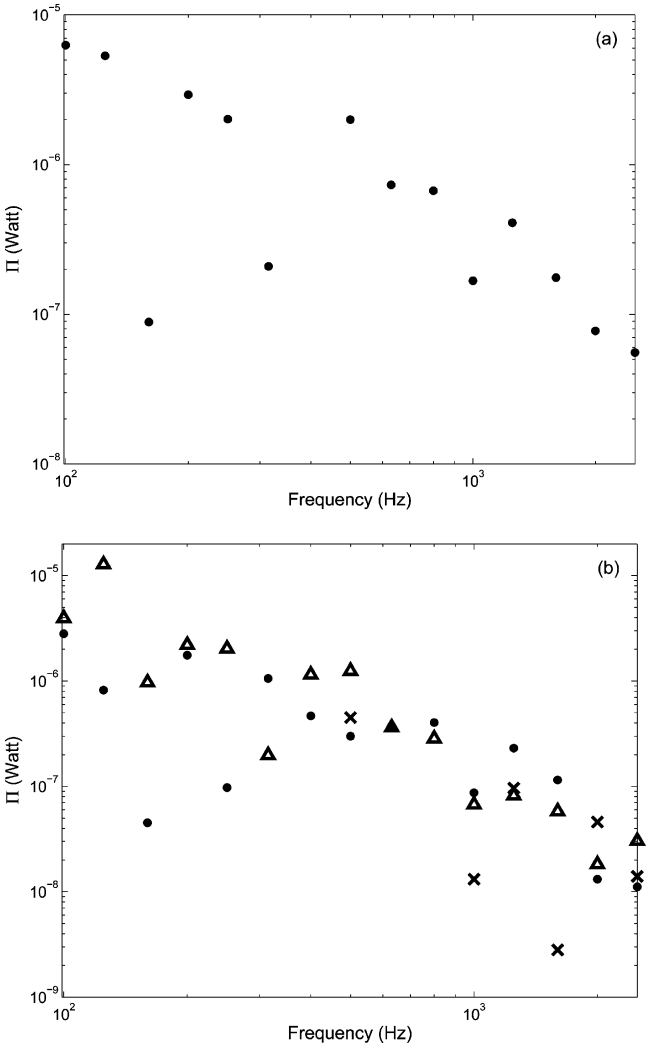

Fig. 13—Power flow through paths (on one third octave band basis): (a) total power flow; (b) power flow through each path. Key: (a) •, total power flow; (b) •, left path; x, center path; Δ, right path. Negative values are not shown here.

comparisons are inappropriate for multi-dimensional motions since the units of Ψ^2 terms are not compatible between translational and rotational directions. Therefore, the weighted mean-square quantity Ψ^2_W that can hold equivalent units for dissimilar motions is employed here to rank order paths along with the driving point mobility Y (or its reciprocal that is the impedance Z), corresponding to force (or velocity) variable, as a weighting factor. The weighted mean-square force (Ψ^2_{WF}) and velocity (Ψ^2_{WV}) are defined as follows:[4]

$$\Psi^2_{WF,i} = \frac{1}{2}\,\mathrm{Re}[F_i F_i^* Y_{ii}] = \frac{|F_i|^2}{2}\,\mathrm{Re}[Y_{ii}] \qquad (17)$$

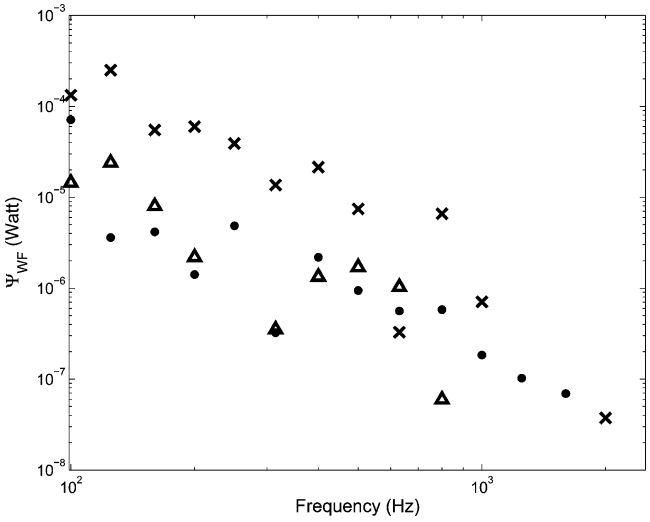

Fig. 14—Weighted mean-square path force (Ψ^2_{WF}) components (on one third octave band basis) for 3 paths. Key: •, left path; x, center path; △, right path. Negative values are not shown here.

$$\Psi^2_{WV,i} = \frac{1}{2}\,\mathrm{Re}[V_i V_i^* Z_{ii}] = \frac{|V_i|^2}{2}\,\mathrm{Re}[Z_{ii}] \qquad (18)$$

The above scalar measures ($\Psi^2_{WF,i}$ and $\Psi^2_{WV,i}$) have the unit of power and are therefore always positive for a linear system since the real parts of driving point mobility and impedance are positive. Note here that Y_{ii} and Z_{ii} are the driving point mobilities and impedances respectively at mount attachment locations of the receiver structure only that is disconnected from paths and source unit. Further, the $\Psi^2_{WF,i}$ (or $\Psi^2_{WV,i}$) represents the power term consisting of force (or moment) and velocity that are induced by the corresponding force (or moment) and velocity in that direction. However, note that $\Psi^2_{WF,i}$ and $\Psi^2_{WV,i}$ do not include any coupling terms unlike the power expression of (14); refer to the article by Singh and Kim[4] for details. The $\Psi^2_{WF,i}$ and $\Psi^2_{WV,i}$ are obtained, as shown in Figs. 14 and 15 respectively, by using measured velocities and the driving point mobilities for our system. Figure 14 shows that the center path is dominant at all frequencies up to 1 kHz (except around 650 Hz), and the left and right paths compete with each other depending on frequencies. The dominance of center path is, however, not observed in Fig. 15. For example, the right path is dominant around 100 Hz but the center path dominates around 300 Hz. Further, negative values are found in the both figures over some frequency ranges such as around 250 Hz at the right path. As explained earlier, this may be due to the missing rotational measurements. Yet, it is conceivable that the running experi-

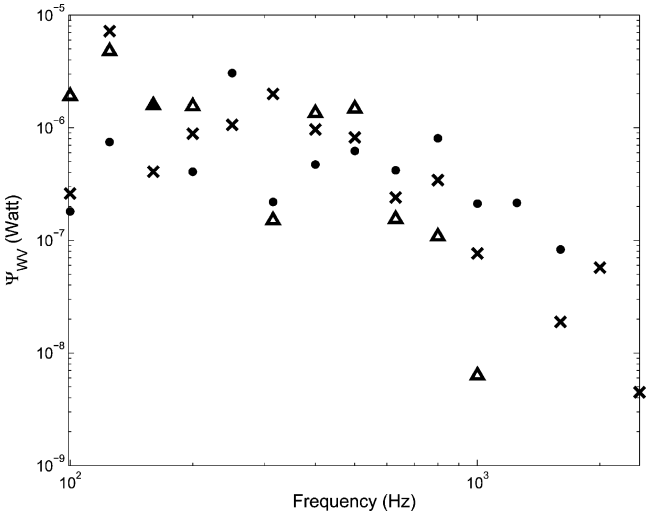

Fig. 15—Weighted mean-square velocity (Ψ^2_{WV}) *components* (*on one third octave band basis*) *for 3 paths. Key: •, left path; x, center path; △, right path. Negative values are not shown here.*

ment deviated from the linear system assumption over those frequency regimes.

7 CONCLUSIONS

Structure-borne noise path measures are experimentally examined using a laboratory multi-path system from 100 to 2800 Hz. The experimental system consists of two chambers and a motor-pump unit that is installed in the source room via three hard mounts. Acoustic and structural frequency response functions are obtained at a number of locations and then operating vibro-acoustic responses are measured for various combinations of source speeds. Only the translational motions in the axial direction of mounts (and normal to the chamber walls) are considered here. First, interfacial path forces are estimated via two indirect methods and are compared with direct force measurements. Results show that the indirect method I (based on the mount driving point data only) yields a closer estimate than the indirect method II (the least-squares type). Second, the paths are rank ordered in terms of the partial sound pressure components in the receiver room. Four alternate rank order schemes are employed to assess the structural noise paths. These schemes include mobility or impedance formulation with either measured path forces or velocities. Finally, alternate energy quantities, including the weighted mean-square force and velocity, are utilized for the rank ordering process.

Table 2 summarizes the path rank orders in terms of the spectrally averaged measures over lower (from 0.1 to 1.0 kHz) and higher (from 1.0 to 2.8 kHz) frequency ranges. Further, rank orders are generated by calculating relative values (shown within the square brackets) with respect to the center path whose measure is assigned as 100% (on a linear basis) or 0 dB (on a logarithmic basis). The center path dominates at lower frequencies in the partial sound pressure calculations based on the mobility or impedance method. However, its dominance is ambiguous when the same methods are compared at higher frequencies. Further, the rank order changes when the impedance formulation is employed (depending upon frequencies of course) although the total sound pressures (as they should) remain the same. This example shows a typical path ranking inconsistency found in real-life problems. For example, the spectral powers show that right path is dominant up to 400 Hz though this result deviates from the ranking found from the partial sound pressure calculations especially when they are based on measured forces. Further, negative values of measured powers (through individual paths) are observed over a wide range of frequencies; an interpretation of such power quantities is not as clear. The weighted mean-square force shows that the center path dominates, that is also illustrated by the partial sound pressure calculations based on measured forces. Nonetheless, the path ranking is not as clear in the weighted mean-square velocity calculations. This may be due to the fact that negative values are found, in some frequency bands, in the weighted mean-square quantities, similar to the power calculations. Overall, the rank order calculations by the partial sound pressures or weighted mean square quantities are found to be formulation-sensitive. The vibration power should have yielded a more inclusive path order, but their partial calculations could include some negative values. Overall, our paper has demonstrated that an experimental study alone (without any rotational measurements) could lead to an ambiguous or inconsistent rank order in some cases and thus some caution must be exercised. Unresolved issues could be resolved by evaluating the effect of missing rotational degrees of freedom on the rank ordering process and power calculations, and by proposing alternate force estimation methods. We have initiated such work and initial results of simpler systems are being reported in companion articles.[11,14] Future work will seek improved estimation techniques and application to the laboratory experiment of this article though the rotational measurements still can not be made.

Table 2—Summary of spectrally averaged path measures in lower (from 0.1 to 1.0 kHz) and higher (from 1.0 to 2.8 kHz) frequency regions.

Measured Quantity	Path Rank Order Measure(s)	Method and Formulation	Path Rank Orders†, ‡, *					
			From 0.1 to 1.0 kHz			From 1.0 to 2.8 kHz		
			LP	CP	RP	LP	CP	RP
Force	Force (N)	Direct Measurement	0.0153 [27%]†	0.0575 [100%]†	0.0135 [23%]†	0.0043 [44%]†	0.0098 [100%]†	0.0053 [54%]†
	Partial Sound Pressure (dB re 20 μPa)	Indirect Estimation (Mobility)	38.5 [−19.0]*	57.5 [0]*	42.0 [−15.5]*	34.5 [−2.5]*	37.0 [0]*	35.5 [−1.5]*
		Indirect Estimation (Impedance)	41.5 [−16.5]*	58.0 [0]*	44.5 [−13.5]*	36.5 [−1.0]*	37.5 [0]*	37.0 [−0.5]*
Velocity	Velocity (μm/s)	Direct measurement	118 [114%]†	81.6 [100%]†	161 [197%]†	41.7 [270%]†	15.4 [100%]†	30.2 [196%]†
	Force (N)	Indirect Method I (Inverse Method)	0.0156 [76%]†	0.0205 [100%]†	0.0102 [50%]†	0.0064 [55%]†	0.0118 [100%]†	0.0067 [57%]†
		Indirect Method II (Least-Squares Method)	0.0210 [39%]†	0.0532 [100%]†	0.0126 [24%]†	0.0040 [16%]†	0.0252 [100%]†	0.0035 [14%]†
	Partial Sound Pressure (dB re 20 μPa)	Indirect Estimation (Mobility)	38.0 [−7.0]*	45.0 [0]*	40.0 [−5.0]*	38.0 [1.0]*	37.0 [0]*	39.0 [2.0]*
		Indirect Estimation (Impedance)	38.0 [−7.0]*	45.0 [0]*	39.5 [−5.5]*	38.5 [0.5]*	38.0 [0]*	38.5 [0.5]*
Force & Velocity	Power (μW)	Direct Measurement (Scalar Product)	0.446 [−68%]‡	−0.652 [100%]‡	1.13 [173%]‡	0.0773 [151%]‡	0.0512 [100%]‡	0.0463 [93%]‡
	Weighted Mean-Square Force (μW)		1.28 [6%]‡	21.9 [100%]‡	1.78 [8%]‡	0.0300 [−48%]‡	−0.0624 [100%]‡	−0.0752 [120%]‡
	Weighted Mean-Square Velocity (μW)		0.696 [78%]‡	0.898 [100%]‡	0.675 [75%]‡	0.0605 [−76%]‡	−0.0793 [100%]‡	−0.0329 [41%]‡

Key †: Relative value in percent (on a linear basis) compared with the center path
Key ‡: Relative value in percent (on a linear basis) compared with the center path when the negative values are also included in the average calculation.
Key *: Relative difference (on a logarithmic basis) compared with the center path

8 ACKNOWLEDGMENTS

The Center for Automotive Research Industrial Consortium at The Ohio State University is gratefully acknowledged for supporting this research since Oct. 2001.

9 REFERENCES

1. L. Cremer and M. Heckl, *Structure-Borne Sound: Structural Vibrations and Sound Radiation at Audio Frequencies*, translated and revised by E. E. Ungar, Springer-Verlag, New York (1973).
2. L. L. Beranek, *Noise and Vibration Control*, revised edition, Institute of Noise Control Engineering, Washington D.C., (1988).
3. S. Kim and R. Singh, "Multi-dimensional characterization of vibration isolators over a wide range of frequencies," *J. Sound Vib.* **245**(5), 877–913 (2001).
4. R. Singh and S. Kim, "Examination of multi-dimensional vibration isolation measures and their correlation to sound radiation over a broad frequency range," *J. Sound Vib.* **262**(3), 419–455 (2003).
5. P. Gardonio, S. J. Elliott, and R. J. Pinnington, "Active isolation of structural vibration on a multiple-degree-of-freedom system Part I: The dynamics of the system,"*J. Sound Vib.* **207**(1), 61-93 (1997).
6. B. A. T. Peterson and B. M. Gibbs, "Use of the source descriptor concept in studies of multi-point and multi-directional vibrational sources," *J. Sound Vib.* **168**(1), 157–176 (1993).
7. LMS International, Application Note. Transfer Path Analysis: The Qualification and Quantification of Vibro-Acoustic Transfer Paths. <http://www.lmsintl.com>
8. M. A. Gehringer, "Application of experimental transfer path analysis and hybrid FRF-based substructuring model to SUV axle noise," SAE Paper 2005-01-1833 (2005).
9. A. Rust and I. Edlinger, "Active path tracking – A rapid method for the identification of structure borne noise paths in vehicle chassis," SAE Paper 2001-01-1470 (2001).
10. H. Douville, P. Masson, and A. Berry, "On-resonance transmissibility methodology for quantifying the structure-borne road noise of an automotive suspension assembly," *Appl. Acoust.*

67(4), 358–382 (2006).
11. A. Inoue, S. Kim, and R. Singh, "Effect of rotational motions on the estimation of interfacial path forces and structure-borne noise path rank orders," Submitted to Applied Acoustics, July (2006).
12. A. N. Thite and D. J. Thompson, "Selection of response measurement locations to improve inverse force determination," *Appl. Acoust.* **67**(8), 797–818 (2006).
13. M. H. A. Janssens and J. W. Verheij, "A pseudo-forces methodology to be used in characterization of structure-borne sound sources," *Appl. Acoust.* **61**(3), 285–308 (2000).
14. A. Inoue, R. Singh, and G. A. Fernandes, "Absolute and relative path measures in a discrete system by using two analytical methods," Submitted to J. Sound and Vib., April (2006).
15. H.-J. Lee and K.-J. Kim, "Multi-dimensional vibration power flow analysis of compressor system mounted in outdoor unit of an airconditioner," *J. Sound Vib.* **272**(3-5), 607–625 (2004).
16. J. Tao and C. M. Mak, "Effect of viscous damping on power transmissibility for the vibration isolation of building services equipment," *Appl. Acoust.* **67**(8), 733–742 (2006).
17. W. L. Li and P. Lavrich, "Prediction of power flows through machine vibration isolators," *J. Sound Vib.* **224**(4), 757–774 (1999).
18. S. Kim and R. Singh, "Structure-borne noise measures and their correlation to sound radiation over a broad range of frequencies," SAE paper 2003-01-1450 (2003).
19. M. A. Sanderson, "Vibration isolation: Moments and rotations included," *J. Sound Vib.* **198**(2), 171–191 (1996).
20. M. A. Sanderson and C. R. Fredo, "Direct measurement of moment mobility, Part II: An experimental study.*J. Sound Vib.* **179**(4), 685–696 (1995).
21. L. H. Ivarsson and M. A. Sanderson, "MIMO technique for simultaneous measurement of translational and rotational mobilities," *Appl. Acoust.* **61**(3), 345–370 (2000).
22. Y. Y. Li and L. Cheng, "Energy transmission through a double-wall structure with an acoustic enclosure: Rotational effect of mechanical links," *Appl. Acoust.*, **67**(3), 185–200 (2006).
23. S. Kim and R. Singh, "Alternate methods for characterizing spectral energy inputs based only on driving point mobilities or impedances," *J. Sound Vib.* **291**(3-5), 604–626 (2006).